Accepted Manuscript

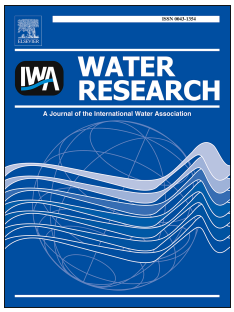

Adsorption of Halogenated Aliphatic Contaminants by Graphene Nanomaterials

Yang Zhou, Onur Guven Apul, Tanju Karanfil

PII: S0043-1354(15)00246-8

DOI: 10.1016/j.watres.2015.04.017

Reference: WR 11246

To appear in: *Water Research*

Received Date: 15 December 2014

Revised Date: 12 April 2015

Accepted Date: 13 April 2015

Please cite this article as: Zhou, Y., Apul, O.G., Karanfil, T., Adsorption of Halogenated Aliphatic Contaminants by Graphene Nanomaterials, *Water Research* (2015), doi: 10.1016/j.watres.2015.04.017.

TOC Art

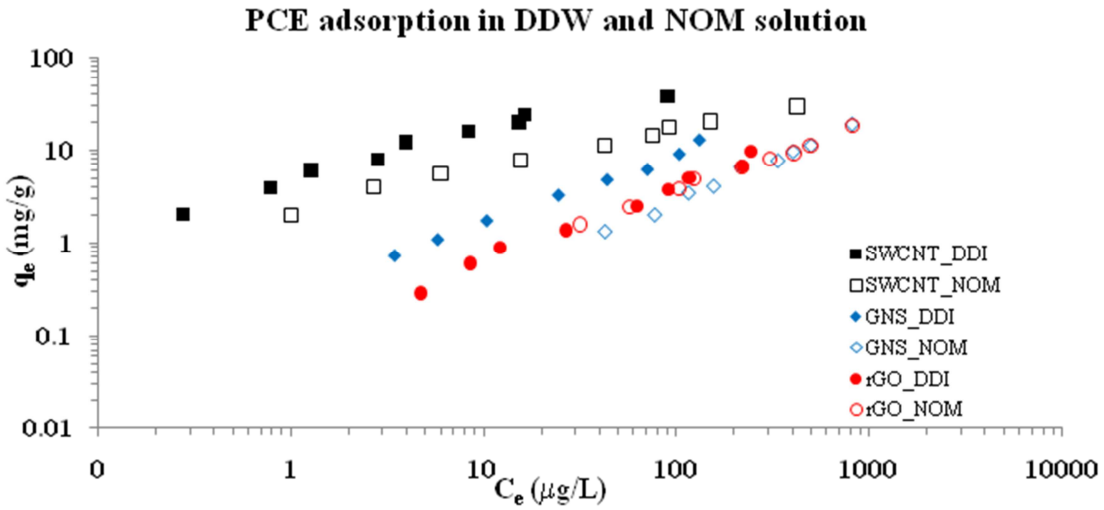

Adsorption of Halogenated Aliphatic Contaminants by Graphene Nanomaterials

Yang Zhou, Onur Guven Apul, Tanju Karanfil*

Department of Environmental Engineering and Earth Sciences
Clemson University
342 Computer Court
Anderson, SC 29625
United States

Submitted to *Water Research*

December 14, 2014

Revised and resubmitted

April 12, 2015

*Corresponding author: email: tkaranf@clemson.edu; phone: +1-864-656-1005; fax: +1-864-656-0672

ABSTRACT

In this study, adsorption of ten environmentally halogenated aliphatic synthetic organic compounds (SOCs) by a pristine graphene nanosheet (GNS) and a reduced graphene oxide (rGO) was examined, and their adsorption behaviors were compared with those of a single-walled carbon nanotube (SWCNT) and a granular activated carbon (GAC). In addition, the impacts of background water components (i.e., natural organic matter (NOM), ionic strength (IS) and pH) on the SOC adsorption behavior were investigated. The results indicated HD3000 and SWCNT with higher microporous volumes exhibited higher adsorption capacities for the selected aliphatic SOCs than graphenes, demonstrating microporosity of carbonaceous adsorbents played an important role in the adsorption. Analysis of adsorption isotherms demonstrated that hydrophobic interactions were the dominant contributor to the adsorption of aliphatic SOCs by graphenes. However, π-π electron donor-acceptor and van der Waals interactions are likely the additional mechanisms contributing to the adsorption of aliphatic SOCs on graphenes. Among the three background solution components examined, NOM showed the most influential effect on adsorption of the selected aliphatic SOCs, while pH and ionic strength had a negligible effects. The NOM competition on aliphatic adsorption was less pronounced on graphenes than SWCNT. Overall, in terms of adsorption capacities, graphenes tested in this study did not exhibit a major advantage over SWCNT and GAC for the adsorption of aliphatic SOCs.

Keywords: Adsorption, Aliphatic Synthetic Organic Compounds, Graphenes, Carbon Nanotubes, Activated Carbons, Natural Organic Matter

1. Introduction

Graphenes are two-dimensional single layered, sp^2 hybridized carbon atoms densely packed as a hexagonal honeycomb lattice and they can be visualized as basic building blocks for fullerenes, carbon nanotubes (CNTs) and graphite [Novoselov et al., 2004]. The unique structure endows graphenes with outstanding mechanical, optical and electronic properties [Geim, 2009; Lee et al., 2008; Novoselov et al., 2005], which make them ideal candidates for a wide range of commercial applications. Commercial production and industrial scale application of graphenes are expected to grow exponentially over the next decades [Geim and Novoselov, 2007; Li and Kraner, 2008]. However, due to their mass production, the release of carbonaceous nanomaterials (such as graphenes) into environment possess various health and environmental risks for plants, animals and humans [Nowack et al. 2012; Upadhyayula et al. 2009; Yu et al. 2014; Zhang et al., 2010; Zhao et al., 2014]. Furthermore, some of the negative impacts might be increased as a result of adsorbing synthetic organic compounds (SOCs) by these nanomaterials, and the fate and transport of SOCs in the environment can be altered.".

Graphenes are hydrophobic nanomaterials with large specific surface areas (SSA); and they have been evaluated as promising adsorbents to remove SOCs from water [Zhao et al et al., 2011; Ramesha et al., 2011; Ji et al., 2013; Sharma and Das, 2013; Zhao et al., 2011; Li et al., 2012; Gao et al., 2012; Li et al., 2013; Apul et al., 2013; Wu et al., 2011]. In our previous study [Apul et al., 2013], graphenes were shown to have higher or comparable adsorption capacities to selected carbon nanotubes and granular activated carbons. In addition, the impact of NOM competition on the adsorption capacity of graphenes was less severe. Therefore, from an engineering perspective, graphenes may serve as novel and alternative adsorbents in engineered treatment system in future [Yu et al. 2015]. To date, the majority of the tested SOCs were aromatic compounds; and no study has examined

the adsorption of aliphatics by graphenes. Several aliphatic SOCs are common organic pollutants that were either regulated by United States Environmental Protection Agency (US EPA) under Priority Pollutants List (e.g., trichloroethylene, tetrachloroethylene, 1,1-dichloroethylene) or listed under Candidate Contaminant List 3 (CCL3) (e.g., 1,1,1,2-tetrachloroethane, 1,1-dichloroethane). Given the paucity of data on this topic in literature, it is important to understand adsorption of aliphatic SOCs by graphenes to adequately assess the environmental impact and engineering applications of graphenes. Therefore, the main objectives of this study were to (i) investigate the factors controlling adsorption of halogenated aliphatic SOCs by graphenes in terms of adsorbent characteristics, adsorbate properties and background solution chemistry, and to (ii) evaluate the application potential of graphenes as alternative adsorbents in treatment systems by comparing their adsorption capacities with those of single-walled carbon nanotubes (SWCNT) and granular activated carbon (GAC).

2. Materials and methods

2.1. Adsorbents

Four carbonaceous adsorbents: pristine graphene nanosheets (GNS, Angstron Materials Inc.), reduced graphene oxide (rGO, Graphenea CO., Ltd.), SWCNT (Chengdu Organic Chemcials Co., Ltd.) and GAC (HD3000, Norit Inc.) were used. GNS, rGO, and SWCNT were used as received from the manufacturers, while HD3000 was ground to 200-325 μm mesh size prior to use. Selected physicochemical properties of the four carbonaceous adsorbents are summarized in Table 1.

2.2. Adsorbates

Ten aliphatic SOCs with different properties were purchased from Acros (PCE, > 99%), Fluka (12DCP, > 99%; 12DBE, > 98%), Matrix Scientific (DBCP, > 98%), Alpha Easer (TCE, > 99.5%), TCI (1112TeCA, > 99%), Baker Analytical (111TCA, > 96.7%) and Sigma Aldrich (112TCA, > 96%; 11DCE, > 99%; CCl_4, > 99.9%). Both of these aliphatic SOCs represented common organic pollutants that were either listed under Priority Pollutants List or CCL3, and they differ in molecular size, hydrophobicity, number of double bonds, and polarizability. Therefore, they were employed as probe molecules to cover some typical adsorbate-adsorbent interactions. Abbreviations, properties and molecular structures of the aliphatic SOCs are summarized in Tables 2 and S1 in Supporting Information.

2.3. NOM solution

The natural organic matter (NOM) was isolated from the influent of Myrtle Beach drinking water treatment plant in South Carolina using a reverse osmosis and followed by resin fractionation, as described elsewhere [Song et al., 2009]. $SUVA_{254}$, defined as the ratio of UV absorbance at 254 nm divided by the dissolved organic carbon (DOC) concentration, is a quantitative measurement of the aromatic content per unit concentration of organic carbon in water [Karanfil et al., 2003]. Natural waters with high $SUVA_{254}$ values (e.g., more than 4.0 L/mg-m) have organic matter with relatively high contents of hydrophobic, aromatic, and high molecular weight components, whereas waters with low $SUVA_{254}$ values (e.g., less than 2.0 L/mg-m) contain mostly non-humic, hydrophilic and low molecular weight material. The

112 $SUVA_{254}$ value of the NOM solution used was around 4.0 L/mg-m, indicating it was rich in
113 aromatic components.

114

115 **2.4. Characterization of adsorbents**

116 Several techniques were used for the characterization of carbonaceous adsorbents.
117 Nitrogen gas adsorption at 77 K was performed with a physisorption analyzer (Micromeritics
118 ASAP 2010) to determine the SSA, total pore volumes (PV) and pore size distributions (PSD) of
119 the four adsorbents. The Brunauer-Emmett-Teller (BET) equation was used to calculate SSA.
120 The total PV were obtained from the adsorbed volume of nitrogen near the saturation point (P/P_0
121 = 0.99). PSD of adsorbents were determined from the nitrogen isotherms using the Density
122 Functional Theory (DFT) model. Oxygen contents of the carbonaceous adsorbents were
123 measured using a Flash Elemental Analyzer 1112 series (Thermo Electron Corporation). In
124 addition, pH of the point of zero charge (pH_{PZC}) of adsorbents was determined using pH
125 equilibration technique. The details about these characterization methods have been provided
126 elsewhere [Dastgheib et al., 2004].

127

128 **2.5. Adsorption experiments**

129 Constant carbon dose aqueous phase isotherm experiments were conducted using
130 completely mixed batch reactors (125 mL glass bottles with Teflon-lined screw caps). Two types
131 of isotherms were conducted at room temperature (20±3 ^{o}C):

132 (1) Distilled and deionized water (DDW) experiments: Concentrated stock solution of
133 each aliphatic SOC was prepared in methanol. Bottles containing about 5 mg of adsorbents were

first filled with DDW and no headspace, and spiked with predetermined volumes of aliphatic SOCs from their methanol stock solutions. For the graphene experiments, the bottles with adsorbents were initially half filled with DDW, sonicated for 20 min, and completely filled with DDW prior to spiking aliphatic SOCs. The volume percentage of the methanol spiked solution per bottle was kept below 0.4% (v/v) to minimize the co-solvent effect. Preliminary kinetic experiments were preformed for TCE adsorption onto four carbonaceous adsorbents; and the results showed that a time period of seven days was sufficient to reach equilibrium (Figure S1). Thus, the bottles with no headspace were placed into a rotary tumbler for one week. The solution pH remained around 6.5 during the experiments. To investigate the effect of pH on adsorption, additional adsorption isotherm experiments were conducted at pH 3 and 11, where the solution pH was adjusted by 0.1 mol/L HCl and NaOH. For ionic strength (IS) effect experiments, the same experimental procedure was used, except the ionic strength was adjusted with NaCl to three levels (IS=0.001, 0.01, 0.1 M). The ranges for pH and ionic strength were kept wider than those typically used in water and wastewater treatment or found in natural water systems to examine their impact in a wider parametric range.

(2) Preloading experiments: The NOM effect on adsorption of aliphatic SOCs by different carbonaceous adsobents was examined under preloading condition, giving an advantage to NOM adsorption prior to that of the SOCs, which represents the most severe NOM competition condition. For the preloading experiments, bottles containing about 5 mg adsorbents were first filled fully with 3 mg DOC/L NOM solution buffered with 1mM $NaH_2PO_4.H_2O/Na_2HPO_4.7H_2O$ and adjusted to pH 7.0, then the bottles with zero headspace were placed into a rotary tumbler. After four days, predetermined volumes of aliphatic SOC stock solutions were directly spiked into the bottles, and then the headspace-free bottles were tumbled

again for an additional week. In NOM preloading experiments, 200 mg/L NaN_3 was added to NOM solution to minimize any biological activity.

After the equilibrium period of isotherm experiments, bottles were placed on a bench overnight to allow settling of the adsorbents, and supernatants of samples in the bottles were transferred to 10 mL centrifuge tube for centrifugation to remove the remaining adsorbents. The supernatants were extracted with hexane by liquid: liquid extraction and analyzed using a gas chromatograph with a micro-electron capture detector (GC-μECD) equipped with a Rxi-624Sil MS Column (Restek, USA). Bottles without any adsorbents served as blanks to monitor the loss of adsorbates during the experiments, which were found to be negligible.

2.6. Isotherm modeling

Four common isotherm models, Freundlich (FM), Langmuir (LM), Langmuir-Freundlich (LFM) and Polanyi-Manes models (PMM), were employed to fit the experimental data. The modeling results showed that FM model resulted in good fits with meaningful parameter values for every case (Tables S2 to S5). Therefore, the FM model was selected to fit the adsorption data in this study:

$$q_e = K_F C_e^n \quad (1)$$

where q_e and C_e represent the solid-phase equilibrium concentration (mg/g) and the liquid-phase equilibrium concentration (μg/L or mg/L), respectively, K_F is the unit-capacity parameter ($(mg/g)/C_e^n$), equal to the amount adsorbed at a value of C_e equal to unity, and n is a dimensionless parameter related to the surface heterogeneity. Two K_F parameters ($K_{F\mu}$ and K_{Fm})

178 were examined for SOCs adsorption capacities at equilibrium concentrations of 1μg/L and
179 1mg/L, respectively.

180

181 **3. Result and discussion**

182 **3.1. Adsorbent characterization**

183 The results of SSA, total PV, PSD, oxygen content and pH_{PZC} of the four carbonaceous
184 adsorbents are summarized in Table 1. The SSA of GNS and rGO were 666 and 497 m^2/g,
185 respectively; and they were considerably smaller than the theoretically calculated SSA of single-
186 layered graphene nanomaterials (2630 m^2/g) [Stoller et al., 2008]. The much lower SSA
187 indicated that graphenes were not present as exposed single-sheets, instead they formed bundles
188 decreasing the SSA. Very high total PV (> 3 cm^3/g) of GNS indicated aggregation may be
189 confining large amounts of space within its 'house-of-cards' like bundle structure. GNS had six
190 times higher total PV than rGO, indicating the oxygen content of rGO may be inhibiting the
191 formation of bulky pores (especially macropores) within its bundle structure. The lacking
192 macropores may also be attributed to tighter aggregation of rGO due to hydrogen bonding
193 between the oxygen containing functional groups within the graphene bundle. When comparing
194 the graphenes with SWCNT and HD3000, no major difference was observed in SSA, total PV
195 and PSD besides the notably large macropore volume of GNS. In addition, rGO had higher
196 oxygen content (17.5%) than other adsorbents as expected, which suggested that the surface of
197 rGO is more hydrophilic. The low pH_{PZC} value of rGO indicated a net negative charge under
198 neutral conditions due to the presence of oxygen-containing functional groups.

199

3.2. The effect of adsorbent properties on adsorption of aliphatics

Adsorption isotherms of PCE, TCE and 1,1-DCE by the four carbonaceous adsorbents in DDW are presented in Figure 1 and the Freundlich isotherm parameters were summarized in Table S6. Some major observations from the isotherms and isotherm parameters are as follow: HD3000 and SWCNT exhibited higher adsorption capacities than graphenes for all aliphatic SOCs tested. The adsorption isotherms were normalized according to the SSA and micropore volumes of adsorbents. However, after normalization, the adsorbed amount of aliphatic SOCs by HD3000 and SWCNT were still higher than those of GNS and rGO (Figures 1-D, E, F, G, H, I). Adsorbents with higher micropore volumes (HD3000 and SWCNT) showed higher adsorption capacities; however, SSA or micropore volume difference did not completely explain the adsorption capacity difference. Because, SSA, total PV and PSD parameters were obtained in the bulk phase of adsorbents via N_2 adsorption, the aggregation of CNTs and graphenes in aqueous phase may change the availability of sorption sites for aliphatic SOCs unlike rigid activated carbon pore structure.

Pristine GNS exhibited higher uptake for the aliphatic SOCs than rGO even after surface area normalization, which was attributed to its low surface polarity. Oxygen-containing functional groups on carbonaceous adsorbents can decrease the accessibility of adsorbents for aliphatic SOCs either through (i) a decrease due to increasing hydrophilicity (i.e. polarity) of the surface, or (ii) a decrease in the number of available adsorption sites due to water cluster formation around the oxygen-containing functional groups. Similar effect of oxygen content of graphenes was also observed on the adsorption of aromatic organic contaminants [Apul et al., 2013].

3.3. The effect of aliphatic SOC properties on adsorption

To investigate the effect of aliphatic SOC properties, adsorption isotherms of the aliphatic SOCs on GNS and rGO are compared in Figures 2-A, B. Hydrophobic interactions are important driving forces for adsorption of SOCs from aqueous solutions. To investigate the contribution of hydrophobicity of the aliphatic SOCs on adsorption, the adsorption isotherms were normalized according to their solubilities (Figures 2-C, D). After the solubility normalization, the separation in the adsorption isotherms on both GNS and rGO were greatly reduced but isotherms did not converge on a single line. This indicates that hydrophobicity of the aliphatic SOCs was an important driving force for adsorption, and there were other factors contributing to adsorption.

To further investigate the effect of the other SOC properties on adsorption, the PCE, TCE and 11DCE isotherms were compared. These compounds have similar molecular structures and configurations but different number of chlorine atoms. As shown in Figures 3-A, B, adsorption affinities of the three aliphatic SOCs by GNS and rGO followed the same order: PCE > TCE > 11DCE. Solubility normalization greatly reduced the differences in the adsorption isotherms, although isotherms did not converge on a single line (Figures 3-C, D), and still followed the same order with smaller differences. The difference in the strengths of π-π electron donor-acceptor (EDA) interactions of these three aliphatics with the graphenes might influence their adsorption. The highly polarizable graphene sheet can play an amphoteric role attracting both π electron-acceptors and π electron-donors to the surface; and chlorine atoms on carbon double bonds of the three SOCs can serve as π electron acceptors, which can involve in adsorption interactions between the SOCs and graphenes through π-π EDA complex formation. Therefore, adsorption affinities of the three aliphatic SOCs by graphenes increase with increasing number of

chlorine atoms. Another possibility influencing adsorption of these three compounds is the nonspecific interactions generally referred to as van der Waals forces. These interactions can exist between molecules regardless of their chemical structures; and they are proportional to the product of polarizability or dipole moment of adsorbates and adsorbents. Thus, stronger van der Waals interactions between PCE and graphenes might occur due to its higher polarizability. The separation in solubility-normalized isotherms of the three aliphatic SOCs on both GNS and rGO were further reduced after polarizability normalization (Figures 3-E, F). This additional reduction suggested that increasing polarizability of aliphatic SOCs may also have positive effects in their adsorption. To further examine the effect of polarizability, two isomer aliphatic SOCs (111TCA and 112TCA) with different polarizability were selected. Figure 4 compares their adsorption isotherms on GNS and rGO after solubility normalization to eliminate the difference in the hydrophobicity of these two compounds. The results showed both GNS and rGO showed higher adsorption capacities for 112TCA than 111TCA. As seen in Table 2, 112TCA has higher polarizability than 111TCA (0.68 vs. 0.41); thus stronger van der Waals interactions between 112TCA and graphenes may be expected.

Presence of π-electrons in the structure of aliphatic SOCs may be another factor affecting their adsorption on graphenes. Aromatic SOCs have strong π-π bonding interactions with graphene surface due to presence of resonating π-electrons in their benzene rings [Apul et al., 2013]. To investigate whether the π-electrons of aliphatic SOCs exert the effect on their adsorption, solubility-normalized adsorption isotherms of PCE vs. 1112TeCA and TCE vs. 112TCA were compared (Figure 5) because they have similar molecular structures but different carbon bonds. After the solubility normalization, the separation between their adsorption isotherms was reduced greatly; and the isotherms almost converged on a single line, which

indicated the π-electrons of aliphatic SOCs might have positive effect on their adsorption by graphenes. Both 1112TeCA and 112TCA were expected to have stronger van der Waals interactions with graphenes than PCE and TCE, respectively due to their higher polarizabilities, which would enhance their adsorption on graphenes. However, after solubility normalization, 1112TeCA and 112TCA did not show higher adsorption affinities to graphenes as compared to PCE and TCE, which therefore indicated that the π-electrons of PCE and TCE possibly contributed to their adsorption on graphenes through π-π EDA complex to counterbalance the contribution of van der Waals interactions to 1112TeCA and 112TCA adsorption. In addition, their solubility-normalized adsorption isotherms once again demonstrated hydrophobic interactions were dominant contributor for the adsorption of aliphatic SOCs on graphenes.

3.4. The effect of background water components on adsorption of aliphatics

3.4.1. The effect of NOM

To investigate the effect of NOM on adsorption of aliphatic SOCs by graphenes and compare NOM effects on adsorption capacities of GNS, rGO and SWCNT, adsorption of six SOCs (PCE, TCE, 11DCE, 112TCA, 1112TeCA, and DBCP) with different properties by GNS, rGO and SWCNT were tested in NOM solution. Their adsorption isotherms in DDW and NOM solutions are presented in Figure 6. Freundlich isotherm parameters in DDI and NOM solution are provided in Table S6 and S7 in Supporting Information, respectively. Two parameters, R_μ and R_m, as the ratios of $K_{F\mu}$ and K_{Fm} in NOM preloading conditions to those in DDW, respectively, were calculated to quantify the effect of NOM on the adsorption of the six aliphatic

290 SOCs by different adsorbents. The lower R_μ and R_m values indicate a greater reduction of
291 adsorption capacity due to NOM preloading.

292 For GNS and rGO, the NOM effect on adsorption capacity of GNS were stronger
293 than rGO, as indicated by lower R_m values of GNS; and rGO exhibited comparable adsorption
294 capacity in the presence of NOM and in DDW as reflected by R_m values of rGO for the six SOCs
295 ranging from 0.72 to 0.91, which can be attributed to electrostatic repulsion of negatively
296 charged NOM molecules and rGO surface. Because the low pH_{PZC} value of rGO (Table 1), it had
297 a net negative charge under neutral pH conditions; and NOM molecules generally carry a net
298 negative charge at the same pH, which would result in less NOM coating on the rGO surface.
299 Furthermore, adsorption of six SOCs by GNS and rGO under NOM preloading conditions was
300 compared to SWCNT adsorption. As shown in Table S7, R_m values of SWCNT for all six SOCs
301 were smaller than those of rGO and GNS, indicating that preloaded NOM exhibited stronger
302 suppression on the adsorption of the aliphatic SOCs by SWCNT. This was attributed to more
303 hindrance of the aliphatic SOC access to the adsorption sites on SWCNT due to the microporous
304 structure of SWCNT bundles in water, in contrast to the flat sheet structure of GNS and rGO.
305 These findings were similar to those of aromatic organic contaminant adsorption, where
306 preloaded NOM exhibited much smaller impact on adsorption capacity of rGO than that of
307 SWCNT [Apul et al., 2013]. However, although preloaded NOM exerted smaller effects on the
308 adsorption capacities of GNS and rGO as compared to SWCNT, graphenes did not exhibit a
309 major advantage, in terms of adsorption capacities, over SWCNT for the adsorption of aliphatic
310 SOCs in the NOM solution (Figure S2).

311 The uptakes of all six SOCs decreased under NOM preloading conditions as reflected by
312 R_m values. However, there were no clear trends observed in R_m values for each SOC; and the R_m

values did not correlate with the SOCs properties such as solubility, molecular size or polarizability. In fact, preloaded NOM did not exert significantly different effects on the six SOCs adsorption in terms of the R_m values. Therefore, for the six aliphatic SOCs, their different physicochemical properties did not cause large differences in NOM effects on their adsorption.

3.4.2. The effect of pH and ionic strength

Three aliphatic SOCs (CCl_4, TCE, and DBCP) with different molecular structure, molecular size and chain lengths were employed as probe molecules to explore the effect of solution pH on adsorption of aliphatic SOCs by graphenes. The adsorption isotherms of CCl_4, TCE and DBCP on GNS and rGO under different pH conditions are presented in Figure S3 in the Supporting Information. The change in pH did not influence the adsorption of these three aliphatic SOCs on GNS and rGO (except for DBCP under pH 11 conditions). Since the tested compounds are non-ionic, their adsorption was independent from solution pH. However, as pH increased, the dissociation of oxygen-containing functional groups on graphene surfaces (especially rGO) also did not show any influence indicating that adsorption of these three aliphatic SOCs occurred on the hydrophobic sites of graphene surface where there were no oxygen-containing functional groups. For DBCP at pH 11, we observed a higher adsorption by graphenes, but actually this does not reflect its real adsorption affinity. Because degradation and transformation of DBCP at high pH might occur during the adsorption experiments indicated by the very low ratio (0.10-0.15) between measured blank concentrations and calculated ones.

To investigate the effect of ionic strength, the same aliphatic SOCs selected for pH experiments were used in the adsorption experiments. Two potential impacts can be observed: (1) increasing ionic strength enhances the activity coefficient of hydrophobic organic

compounds, leading to a decrease in their solubility (i.e. salting out effect), which is favorable for SOCs adsorption [Zhang et al., 2010]; and (2) the ions may penetrate into the diffuse double layer surrounding the graphene surfaces and eliminate the repulsive energy between the adsorbents, facilitating the formation of a more compact aggregation structure (i.e. squeezing-out), which is unfavorable for SOCs adsorption [Zhang et al., 2010]. Increasing ionic strength had negligible effect on adsorption of the aliphatic SOCs by both GNS and rGO (Figure S3). Therefore, the results indicated that either the contribution of salting-out effect to the adsorption of these aliphatic SOCs was equivalent to that of the squeezing-out effect or both the salting-out effect and squeezing-out effect were too weak to influence the adsorption of the SOCs on graphenes.

4. Conclusions

Graphene nanomaterials adsorbed halogenated aliphatic SOCs, however the overall adsorption capacities of graphene nanomaterials were smaller than those of carbon nanotubes and activated carbon in the presence of NOM. Hydrophobicity was the dominant contributor for the adsorption of aliphatic SOCs on graphenes, but it was not the only mechanism controlling the adsorption, π-π EDA interaction and van der Waals interaction appear to be the additional mechanisms contributing to the adsorption of aliphatic SOCs on graphenes. It should be noted that these adsorption interactions were observed for the selected halogenated aliphatic contaminants with comparable molecular configuration and sizes in this study. Further research is warranted to confirm and extend the findings to larger and more complex aliphatic molecules or different classes of contaminants. Among the three background water characteristics examined, NOM showed the most important effect on adsorption, whereas the changes in pH and ionic strength had a negligible effect on the

adsorption of selected halogenated aliphatic SOCs. NOM preloading exerted minimal effect on adsorption capacities of rGO for aliphatic SOCs, which was attributed to low degree of NOM coating on rGO surface due to electrostatic repulsion between negatively charged NOM molecules and rGO. NOM exhibited severe suppression on adsorption capacities of SWCNT than those of graphenes. This was attributed to microporous structure of SWCNT aggregates as compared with flat sheet structure of graphenes. In terms of adsorption capacities, graphenes did not exhibit a major advantage over SWCNT and HD3000 for the adsorption of aliphatic SOCs. Future studies also need to examine adsorption kinetics to assess whether graphenes exhibit advantages over other carbonaceous adsorbents for halogenated aliphatic SOCs.

Acknowledgement

This work was supported by a research grant from the National Science Foundation (CBET 0967425). However the manuscript has not been subjected to the peer and policy review of the agency and therefore does not necessarily reflect it views.

374 **References**

375

376 Apul, O.G., Wang, Q.L., Zhou, Y., Karanfil, T. 2013. Adsorption of aromatic organic
377 contaminants by graphene nanosheets: comparison with carbon nanotubes and activated
378 carbon. Water Research 47 (4), 1648-1654.

379

380 Carter, M.C., Kildfuff, J.E., Weber Jr, W.J. 1995. Site energy distribution analysis of preloaded
381 adsorbent. Environmental Science and Technology 29 (7), 1773-1780.

382

383 Chen, J., Chen, W., Zhu, D. 2008. Adsorption of nonionic aromatic compounds to single-walled
384 carbon nanotubes: Effects of aqueous solution chemistry. Environmental Science and
385 Technology 42 (19), 7225-7230.

386

387 Dastgheib, S.A., Karanfil, T., Cheng, W. 2004. Tailoring activated carbons for enhanced removal
388 of natural organic matter from natural waters. Carbon 42 (3), 547-557.

389

390 Fontecha-Camara, M.A., Lopez-Ramon, M.V., Alvarez-Merine, M.A., Morene-Castilla, C. 2007.
391 Effect of surface chemistry, solution pH, and ionic strength on the removal of herbicides
392 diuron and amitrole from water by an activated cabon fiber. Langmuir 23 (3), 1242-1247.

393

394 Gao, Y., Li, Y., Zhang, L., Huang, H., Hu, J.J., Shah, S.M., Su, X.G. 2012. Adsorption and
395 removal of tetracycline antibiotics from aqueous solution by graphene oxide. Journal of
396 Colloid and Interface Science 368 (1), 540-546.

397

398 Geim, A.K., 2009. Graphene: status and prospects. Science 324 (5934), 1530-1534.

399

400 Geim, A.K., Novoselov, K.S. 2007. The rise of graphene. Nature Materials 6 (3), 183-191.

401

Giles, R.G.F., Green, I.R., Oosthuizen, F.J., Taylor, C.P. 2003. Syntheses of asymmetric 2-benzopyrans. The influence of aromatic halogen substituents on the intramolecular cyclisation of enantiopure tethered phenolic lactaldehydes. Archive for Organic Chemistry 2002 (9), 99-116.

Ji, L.L., Chen, W., Xu, Z.Y., Zheng, S.R., Zhu, D.Q. 2013. Graphene Nanosheets and graphite oxide as promising adsorbents for removal of organic contaminants from aqueous solution. Journal of Environmental Quality 42 (1), 191-198.

Karanfil, T., Erdogan, I., Schlautman, M.A. 2003. Selecting filter membranes for measuring DOC and UV254. Journal of American Water Works Association, 95, (3) 86-100.

Karanfil, T., Dastgheib, S.A. 2004. Trichloroethylene adsorption by fibrous and granular activated carbons: Aqueous phase, gas phase and water vapor adsorption studies. Environmental Science and Technology 38 (22), 5834-5841.

Lee, C., Wei, X., Kysar, J.W., Hone, J. 2008. Measurement of the elastic properties and intrinsic strength of monolayer graphene. Science 321 (5887), 385-388.

Li, D., Kaner, R.B., 2008. Graphene-based materials. Science 320 (5880), 1170-1171.

Li, L., Quinlivan, P.A., Knappe, D.R.U.] 2002. Effects of activated carbon surface chemistry and pore structure on the adsorption of organic contaminants from aqueous solution. Carbon 40 (12), 2085-2100.

Li, Y.H., Du, Q.J., Liu, T.H., Peng, X.J., Wang, J.J., Sun, J.K., Wang, Y.H., Wu, S.L., Wang, Z.H., Xia, Y.Z., Xia, L.H.] 2013. Comparative Study of methylene blue dye adsorption onto activated carbon, graphene oxide, and carbon nanotubes. Chemical Engineering Research and Design 91 (2), 361-368.

Li, Y.H., Du, Q.J., Liu, T.H., Sun, J.K., Jiao, Y.Q., Xia, Y.Z., Xia, L.H., Wang, Z.H., Zhang, W., Wang, K.L., Zhu, H.W., Wu, D.H. 2012. Equilibrium, kinetic and thermodynamic studies on the adsorption of phenol onto graphene. Materials Research Bulletin 47 (8), 1898-1904.

Lin, D., Xing, B. 2008. Adsorption of phenolic compounds by carbon nanotubes: Role of aromaticity and substitution of hydroxyl groups. Environmental Science and Technology 42 (19), 7254-7259.

Lu, C.S., Chung, Y.L., Chang, K.F. 2005. Adsorption of trihalomethanes from water with carbon nanotubes. Water Research 39 (6), 1183-1189.

Novoselov, K.S., Geim, A.K., Morozov, S.V., Jiang, D., Zhang, Y., Dubonos, S.V., Grigorieva, I.V., Firsov, A.A. 2004. Electric field effect in atomically thin carbon films. Science 306 (5696), 666-669.

Novoselov, K.S., Jiang, D., Schedin, F., Booth, T.J., Khotkevich, V.V., Morozov, S.V., Geim, A.K. 2005. Two-dimensional atomic crystals. Proceedings of the National Academy of Sciences 102 (30), 10451-10453.

Nowack, B., Ranville, J.F., Diamodn, S., Gellego-Urrea, J.A., Metcalfe, C., Rose, J., Horne, N., Koelmans, A.A., Klaine, S.J. 2012. Potential scenarios for nanomaterial release and subsequent alteration in the environment. Environmental Toxicology and Chemistry 31 (1), 50-59.

Ramesha, G.K., Vijaya Kumara, A., Muralidhara, H.B., Sampath, S. 2011. Graphene and graphene oxide as effective adsorbents toward anionic and cationic dyes. Journal of Colloid and Interface Science 361 (1), 270-277.

Robin, G. F. Giles.; Ivan, R. Green.; Francois, J. Oosthuizen.; C. Peter Taylor. 2002. Syntheses of asymmetric 2-benzopyrans. The influence of aromatic halogen substituents on the

463 intramolecular cyclisation of enantiopure tethered phenolic lactaldehydes. Archive for
464 Organic Chemistry (9), 99-116.

465

466 Sharma, P., Das, M.R. 2013. Removal of a cationic dye from aqueous solution using graphene
467 oxide nanosheets: investigation of adsorption parameters. Chemical Engineering Journal
468 58 (1), 151-158.

469 Song, H., Orr, O., Hong, Y., Karanfil, T. 2009. Isolation and fractionation of natural organic
470 matter: evaluation of reverse osmosis performance and impact of fractionation
471 parameters. Environmental Monitoring and Assessment 153 (1), 307-321.

472

473 Stoller, M.D., Park, S.J., Zhu, Y.,W., An, J.,H., Ruoff, R.S. 2008. Graphene-based
474 ultracapacitors. Nano Letters 8 (10), 3498-3502.

475 Upadhyayula, V.K.K., Deng, S., Mitchell, M.C., Smith, G.B. 2009. Application of carbon
476 nanotube technology for removal of contaminants in drinking water: A review. Science
477 of the Total Environment 408 (1), 1-13.

478 Wu, T., Cai, X., Tan, S.Z., Li, H.Y., Liu, J.S., Yang, W.D. 2011. Adsorption characteristics of
479 acrylonitrile, P-toluenesulfonic acid, 1-naphthalenesulfonic acid and methylene blue on
480 graphene in aqueous solutions. Chemical Engineering Journal 173 (1), 144-149.

481

482 Yang, K., Wu, W.H., Jing, Q.F., Zhu, L.Z. 2008. Aqueous adsorption of aniline phenol, and their
483 substitutes by multi-walled carbon nanotubes. Environmental Science and Technology 42
484 (21), 7931-7936.

485

486 Yang, K., Xing, B. 2009. Adsorption of fulvic acid by carbon nanotubes from water.
487 Environmental Pollution 157 (4), 1095-1100.

488 Yu, J.G., Zhao, X.H., Yang, H., Chen, X.H., Yang, Q., Yu, L.Y., Jiang, J.H., Chen, X.Q. 2014.
489 Aqueous adsorption and removal of organic contaminants by carbon nanotubes. Science
490 of the Total Environment 482-483, 241-251.

491 Yu, J.G., Yu, L.Y., Yang, H., Liu, Q., Chen, X.H., Jiang, X.Y., Chen, X.Q., Jiao, F.P. 2015.
492 Graphene nanosheets as novel adsorbents in adsorption, preconcentration and removal of
493 gases, organic compounds and metal ions. Science of the Total Environment 502, 70-79.

494 Zhang, S., Shao, T., Kose, H.S., Karanfil, T. 2010. Adsorption of aromatic compounds by
495 carbonaceous adsorbents: A comparative study on granular activated carbon, activated
496 carbon fiber, and carbon nanotubes. Environmental Science and Technology 44 (16),
497 6377-6383.

498

499 Zhang, S.J., Shao, T., Bekaroglu, S.S.K., Karanfil, T. 2010. Adsorption of synthetic organic
500 chemicals by carbon nanotubes: Effects of background solution chemistry. Water
501 Research 44 (6), 2067-2074.

502

503 Zhang, Y., Ali, S.F., Dervishi, E., Xu, Y., Li, Z., Casciano, D., Biris, A.S. 2010. Cytotoxicity
504 effects of graphene and single-wall carbon nanotubes in neural phaeochromocytoma-
505 derived PC12 cells. Journal of the American Chemical Society 4 (6), 3181-3186.

506

507 Zhao, G., Jiang, L., He, Y., Li, J., Dong, H., Wang, X., Hu, W. 2011. Sulfonated graphene for
508 persistent aromatic pollutant management. Advanced Materials 23 (34), 3959-3963.

509

510 Zhao, G.X., Li, J.X., Wang, X.K. 2011. Kinetic and thermodynamic study of 1-naphthol
511 adsorption from aqueous solution to sulfonated graphene nanosheets. Chemical
512 Engineering Journal 173 (1), 185-190.

513

514 Zhao, J., Wang, Z.Y., White, J.C., Xing, B.S. 2014. Graphene in the aquatic environment:
515 adsorption, dispersion, toxicity and transformation. Environmental Science and
516 Technology 48 (17), 9995-10009.

517

518

519 **Table 1.** Physicochemical properties of adsorbents

Adsorbent	SSA_{BET} [a]	V_T [b]	DFT Pore Volume Distribution [c]			Oxygen Content	pH_{pzc}
			V_{micro} (< 2 nm)	V_{meso} (2-50nm)	V_{macro} (> 50nm)		
	m^2/g	cm^3/g	cm^3/g, (%)	cm^3/g, (%)	cm^3/g, (%)	%	
GNS	666	3.138	0.065, (2.1)	1.196, (38.1)	1.877, (59.8)	0.8	9.8
rGO	497	0.530	0.081, (15.3)	0.377, (71.1)	0.072, (13.6)	17.5	4.1
SWCNT	537	1.240	0.117, (9.4)	0.581, (46.9)	0.542, (43.7)	0.9	7.5
HD3000	642	0.775	0.108, (13.9)	0.449, (57.9)	0.218, (28.1)	3.4	6.9

520 [a] Specific surface area calculated with the Brunauer-Emmett-Teller (BET) model, [b] Total pore volume calculated from single point adsorption at $P/P_0 = 0.99$, [c] Pore
521 volume in each pore size range obtained from the density functional theory (DFT) analysis.

522 **Table 2.** Selected properties of aliphatic SOCs

SOC	Abbreviation	MW[a] g/mol	Density g/cm^3	MV[b] cm^3/mol	C_S[c] mg/L	LogK_{OW}[d]	Polarizability[e]
trichloroethylene	TCE	131	1.46	89.7	1183	2.42	0.37
tetrachloroethylene	PCE	166	1.62	102.5	224	3.40	0.44
1,1,1-trichloroethane	111TCA	133	1.32	100.8	1358	2.49	0.41
1,1,2-trichloroethane	112TCA	133	1.44	92.4	4483	1.89	0.68
carbon tetrachloride	CCl_4	154	1.59	96.9	790	2.83	0.38
1,1-dichloroethylene	11DCE	97	1.21	80.2	2375	1.32	0.34
1,2-dichloropropane	12DCP	113	1.16	97.4	2819	2.28	0.68
1,2-dibromoethane	12DBE	188	2.17	86.6	4177	1.96	0.76
1,1,1,2-tetrachloroethane	1112TeCA	168	1.55	108.3	1103	2.93	0.63
1,2-dibromo-3-chloropropane	DBCP	236	2.08	113.5	985	2.43	0.78

523 [a] molecular weight; [b] molar volume; [c] water solubility at 25 ^oC obtained from the Material Safety Data Sheet of each compound; [d] octanol-water partitioning coefficient
524 simulated with ACDLABS11.0 (ChemSketch and ACD/3D Viewer); [e] polarizability obtained from ACD/ADME Suite 5.0.

525

526

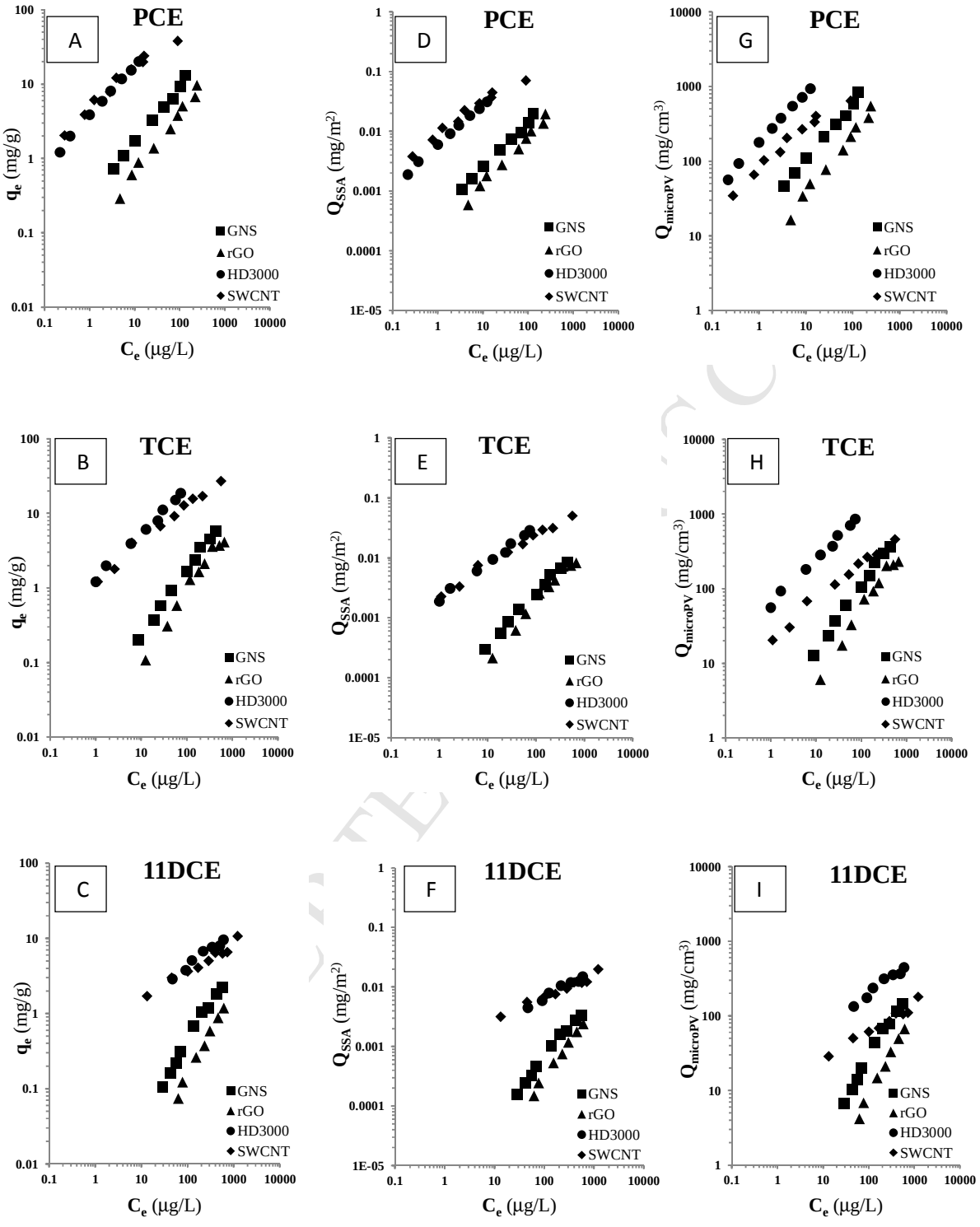

Figure 1. Adsorption isotherms in DDW (A) PCE mass basis, (B) TCE mass basis, (C) 11DCE mass basis, (D) PCE surface area normalized, (E) TCE surface area normalized, (F) 11DCE surface area normalized, (G) PCE micropore volume normalized, (H) TCE micropore volume normalized, and (I) 11DCE micropore volume normalized.

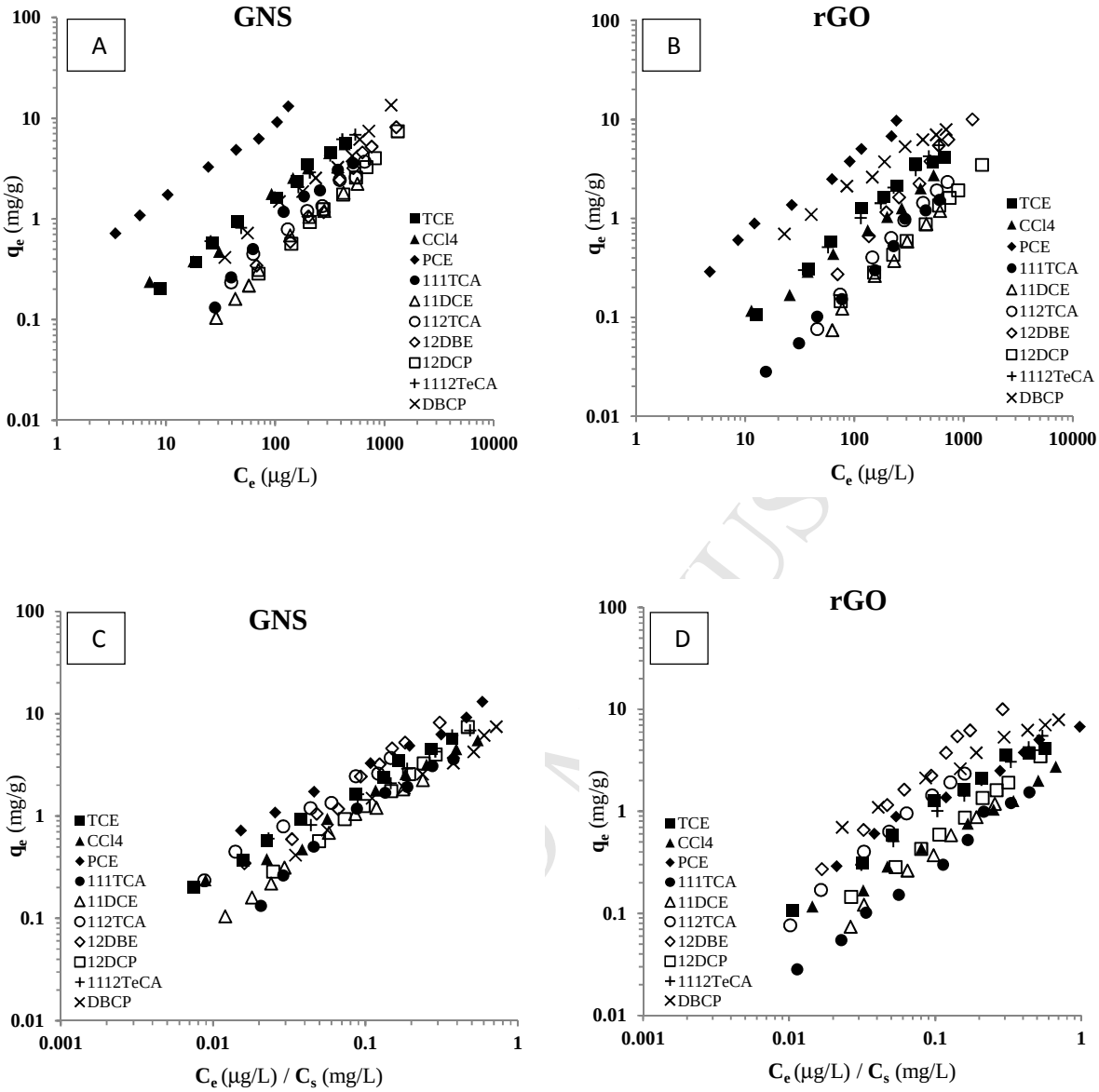

Figure 2. Adsorption isotherms of ten aliphatic SOCs by GNS and rGO in DDW (A) GNS mass basis, (B) rGO mass basis, (C) GNS solubility normalized, (D) rGO solubility normalized .

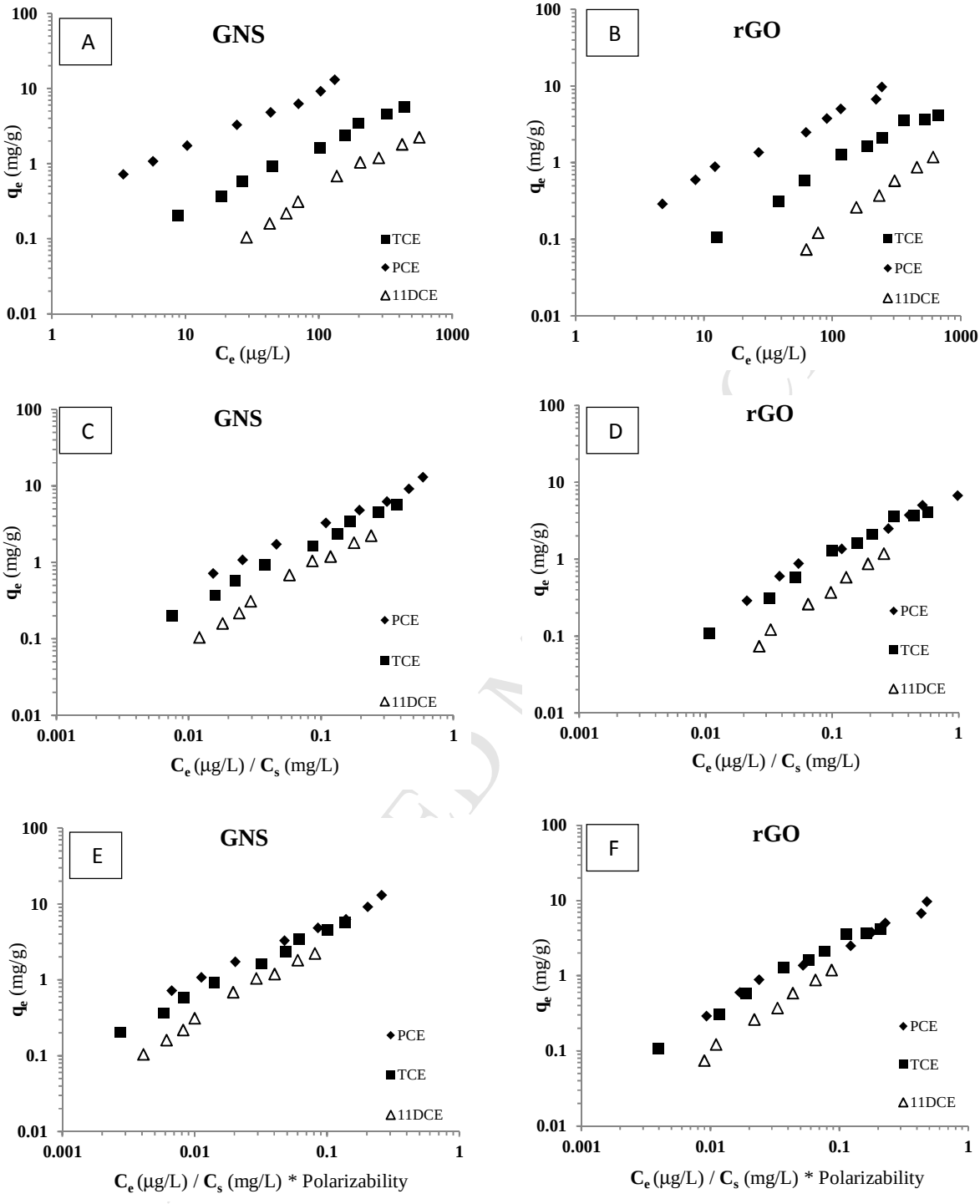

Figure 3. Adsorption isotherms of PCE, TCE and 11DCE in DDW (A) GNS mass basis, (B) rGO mass basis, (C) GNS solubility normalized, (D) rGO solubility normalized, (E) GNS polarizability normalized, and (F) rGO polarizability normalized.

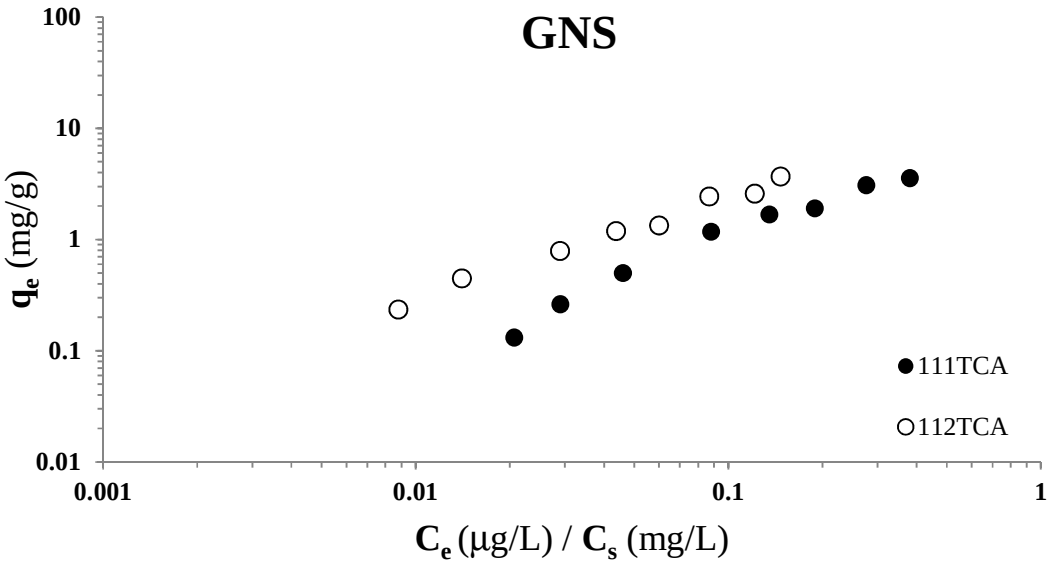

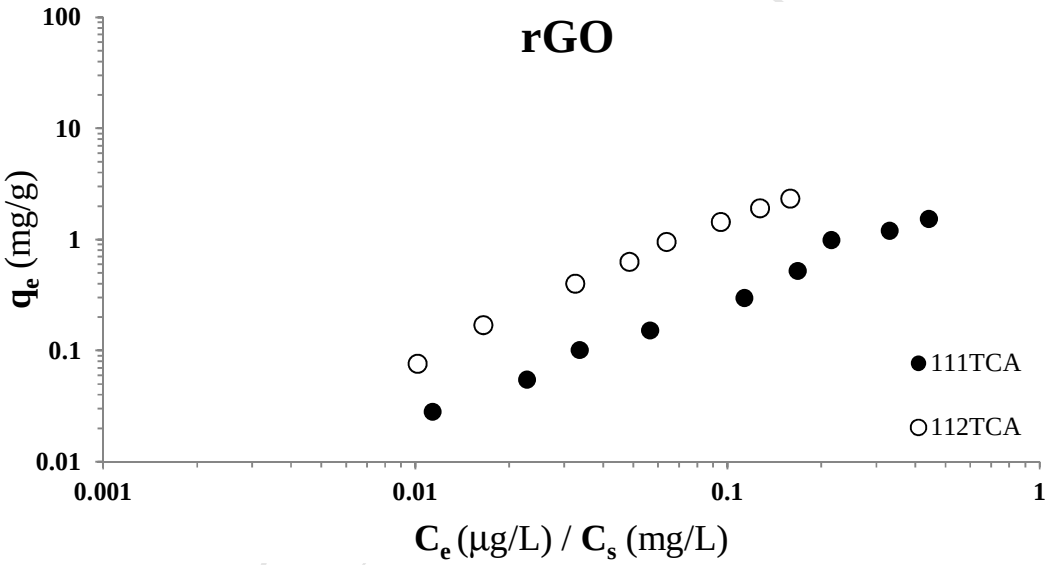

Figure 4. Comparison of 111TCA and 112TCA solubility-normalized adsorption isotherms on GNS and rGO in DDW.

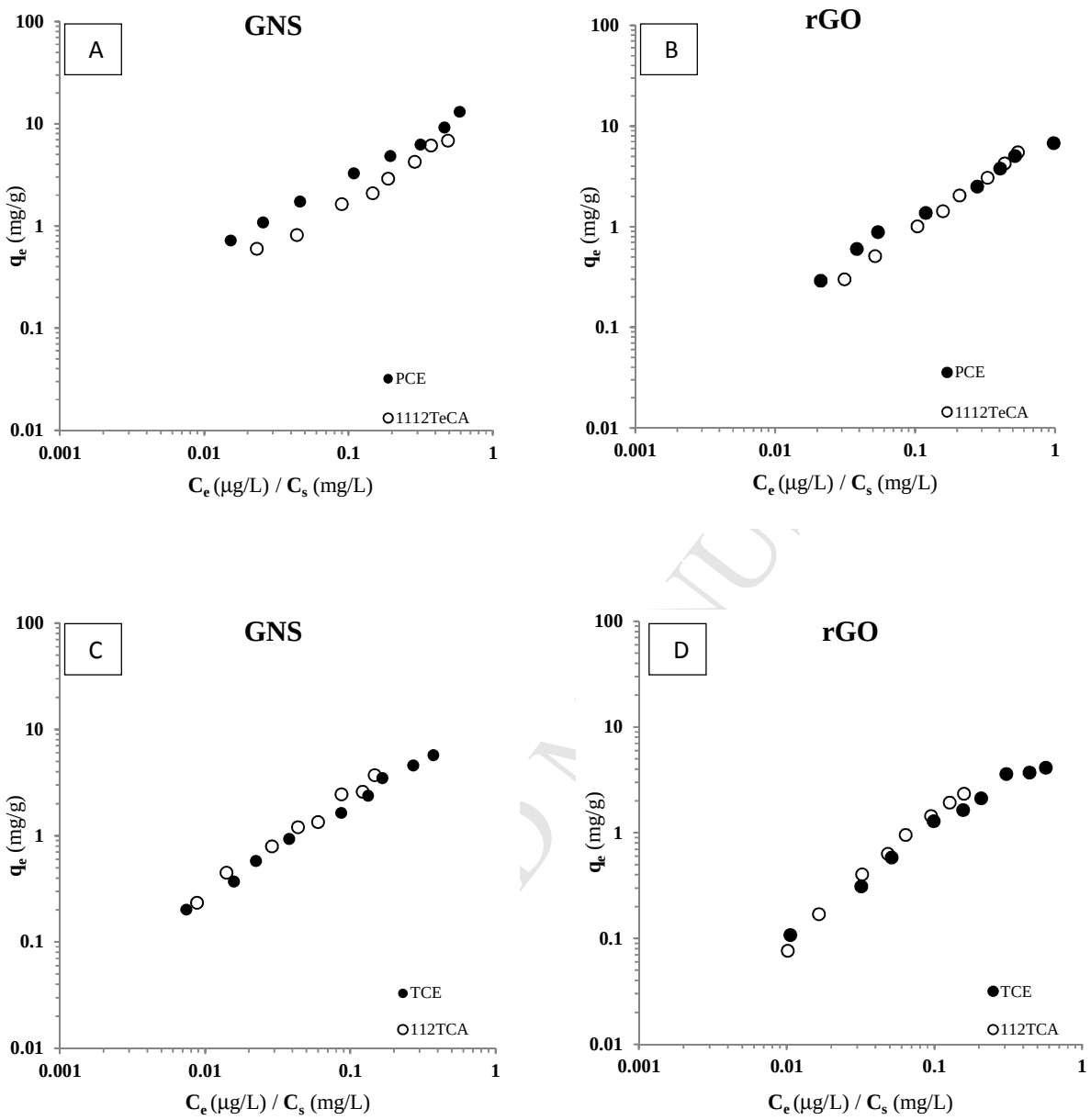

558

559

560

561 **Figure 5.** Comparison of PCE vs. 1112TeCA and TCE vs. 112TCA solubility normalized adsorption
562 isotherms on GNS and rGO in DDW (A) PCE vs. 1112TeCA-GNS, (B) PCE vs. 1112TeCA-rGO, (C)
563 TCE vs. 112TCA-GNS, and (D) TCE vs. 112TCA- rGO.

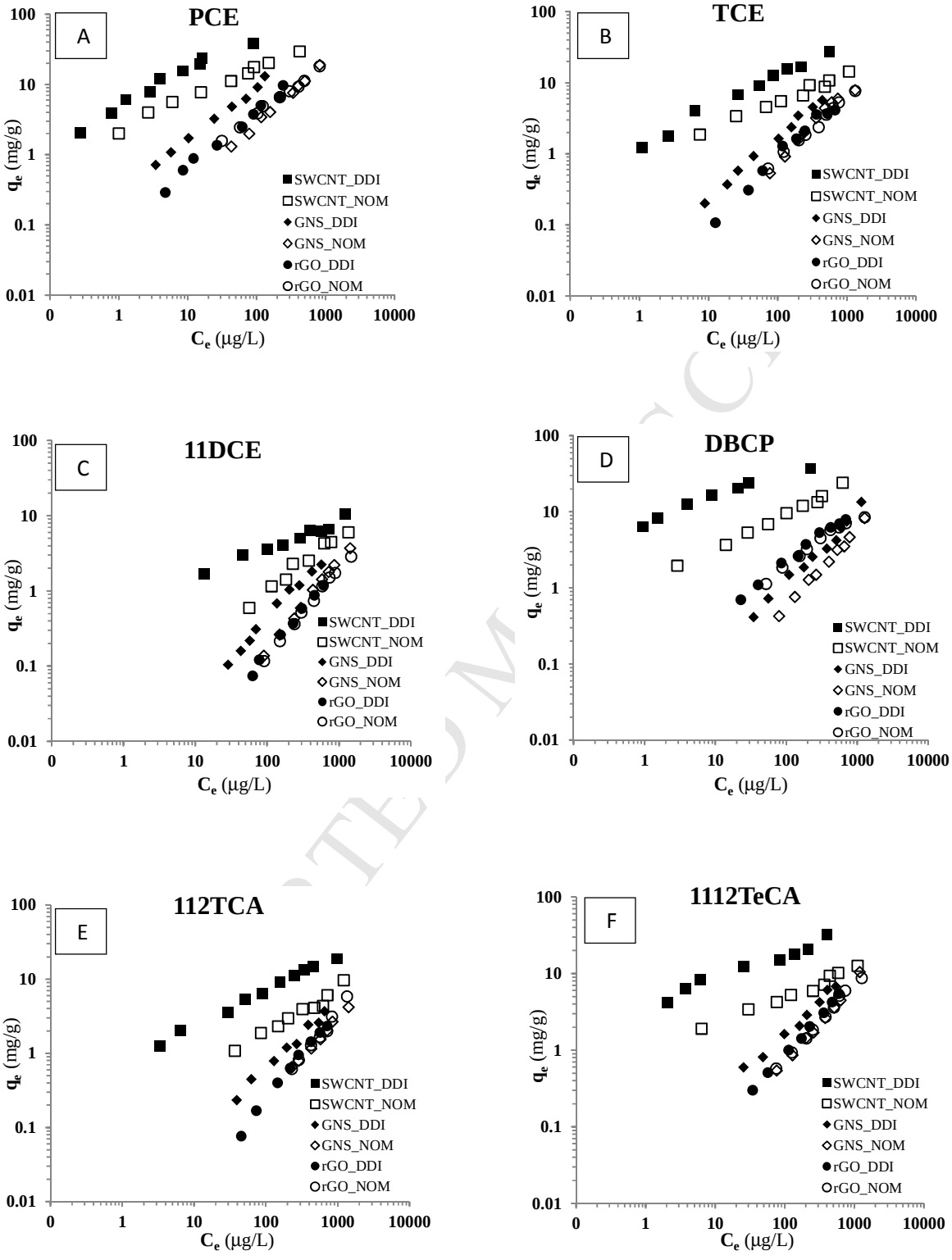

Figure 6. Adsorption isotherms in DDW and under NOM preloading conditions (A) PCE, (B) TCE, (C) 11DCE, (D) DBCP, (E) 112TCA, and (F) 1112TeCA.

Highlights

- Graphene nanomaterials adsorb halogenated aliphatic SOCs
- The effect of NOM was smaller on adsorption capacity of graphenes than CNTs
- rGO showed comparable adsorption capacities in NOM solution and DDW
- Hydrophobicity was the dominant factor in the adsorption of tested aliphatic SOCs by graphenes
- CNTs and GAC exhibited higher adsorption capacities for aliphatic SOCs than graphenes

SUPPORTING INFORMATION

for

Adsorption of Halogenated Aliphatic Contaminants by Graphene Nanomaterials

Yang Zhou, Onur Guven Apul, Tanju Karanfil*

Department of Environmental Engineering and Earth Sciences
Clemson University
342 Computer Court
Anderson, SC 29625
United States

*Corresponding author: email: tkaranf@clemson.edu; phone: +1-864-656-1005; fax: +1-864-656-0672

25 **Table S1.** Molecular structures of selected aliphatic SOCs

SOC	Abbreviation	Molecular Structures
trichloroethylene	TCE	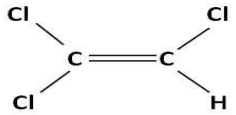
tetrachloroethylene	PCE	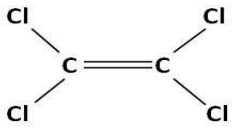
1,1,1-trichloroethane	111TCA	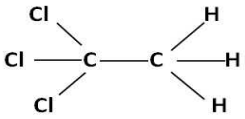
1,1,2-trichloroethane	112TCA	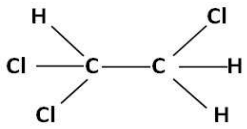
carbon tetrachloride	CCl_4	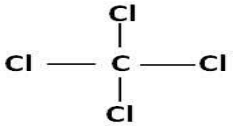
1,1-dichloroethylene	11DCE	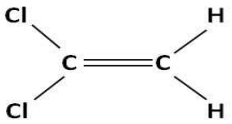
1,2-dichloropropane	12DCP	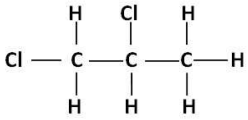
1,2-dibromoethane	12DBE	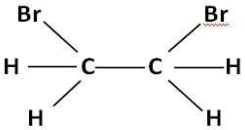
1,1,1,2-tetrachloroethane	1112TeCA	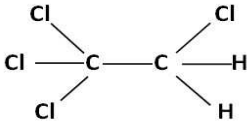
1,2-dibromo-3-chloropropane	DBCP	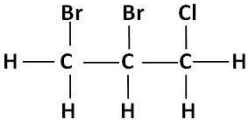

Table S2. Nonlinear model fits for adsorption of ten aliphatic SOCs on GNS

SOC	Langmuir				Freundlich				Langmuir-Freundlich					Polanyi-Manes models				
	q_m	K_L	r^2	RMSE	K_F	n	r^2	RMSE	q_m	K_S	n	r^2	RMSE	q_m	a	b	r^2	RMSE
TCE	16.8	0.001	0.993	0.17	0.032	0.86	0.996	0.20	17.4	0.001	0.991	0.993	0.19	9.8	-24.7	1.26	0.993	0.19
CCl_4	13.7	0.002	0.999	0.08	0.039	0.82	0.984	0.14	13.8	0.002	0.996	0.999	0.08	7.3	-29.1	1.28	0.999	0.08
PCE	129.2	0.001	0.976	0.74	0.287	0.75	0.995	0.65	1370.4	4E-05	0.877	0.981	0.72	65.5	-5.3	0.45	0.995	0.38
111TCA	13.2	0.001	0.989	0.15	0.005	1.09	0.982	0.17	7.1	0.002	1.223	0.991	0.14	5.3	-66.9	1.57	0.991	0.14
11DCE	10.1	0.001	0.994	0.06	0.003	1.05	0.990	0.08	5.1	0.001	1.180	0.996	0.06	4.1	-43.3	1.59	0.996	0.05
112TCA	35.5	2E-04	0.971	0.22	0.009	0.93	0.987	0.22	110.6	4E-05	0.948	0.972	0.24	48.6	-10.9	0.74	0.973	0.23
12DBE	424.1	2E-05	0.982	0.37	0.002	1.15	0.983	0.36	424.1	2E-05	1.054	0.984	0.38	13.1	-120.7	1.83	0.993	0.24
12DCP	951.1	5E-06	0.980	0.34	0.003	1.10	0.997	0.10	951.2	1E-05	1.195	0.998	0.12	27.2	-13.2	0.78	0.999	0.06
1112TeCA	45.8	3E-04	0.985	0.31	0.035	0.84	0.987	0.31	49.2	3E-04	0.993	0.985	0.34	12.7	-22.5	1.07	0.985	0.34
DBCP	1905.4	6E-06	0.974	0.68	0.017	0.92	0.985	0.48	1905.5	1E-05	1.172	0.987	0.52	20.0	-6.3	0.53	0.996	0.33

q_m (mg/g): maximum adsorption capacity; K_L(L/μg): adsorption affinity coefficient; r^2: coefficient of determination; RMSE: residual root mean square error; K_F [(mg/g)/(μg/L)^n]: adsorption affinity coefficient; n: nonlinear index; K_S [(L/μg)^n]: adsorption affinity coefficient; a and b:fitting parameters; underlined numbers represent the unreasonable values of the models.

Table S3. Nonlinear model fits for adsorption of ten aliphatic SOCs on rGO

SOC	Langmuir				Freundlich				Langmuir-Freundlich					Polanyi-Manes models				
	q_m	K_L	r^2	RMSE	K_F	n	r^2	RMSE	q_m	K_S	n	r^2	RMSE	q_m	a	b	r^2	RMSE
TCE	8.7	0.001	0.974	0.26	0.011	0.95	0.984	0.34	5.5	0.003	1.430	0.981	0.24	4.6	-112.4	1.84	0.980	0.25
CCl_4	93.0	6E-05	0.992	0.09	0.014	0.82	0.992	0.08	93.0	5E-05	0.961	0.993	0.09	5.6	-8.3	0.70	0.998	0.04
PCE	38.8	0.001	0.963	0.66	0.096	0.82	0.989	0.64	398.1	5E-05	0.860	0.966	0.69	6.9	-26.4	1.19	0.995	0.28
111TCA	29.6	9E-05	0.972	0.10	0.001	1.13	0.991	0.10	2.1	0.003	1.860	0.982	0.09	2.0	-208.1	1.87	0.981	0.09
11DCE	203.3	9E-06	0.991	0.04	0.001	1.18	0.992	0.02	203.3	2E-05	1.122	0.997	0.03	3.8	-26.1	1.21	0.998	0.02
112TCA	178.1	2E-05	0.994	0.07	0.001	1.24	0.994	0.05	178.1	3E-05	1.075	0.997	0.06	5.9	-79.6	1.70	0.999	0.02
12DBE	998.3	8E-06	0.973	0.57	0.001	1.30	0.991	0.47	998.3	1E-05	1.132	0.982	0.50	17.7	-123.4	1.82	0.990	0.38
12DCP	303.3	7E-06	0.991	0.11	0.001	1.07	0.998	0.05	303.3	1E-05	1.114	0.998	0.05	7.5	-18.4	0.95	0.998	0.05
1112TeCA	607.4	1E-05	0.997	0.12	0.009	1.00	0.999	0.09	607.4	2E-05	1.059	0.998	0.10	13.4	-13.7	0.82	0.999	0.07
DBCP	13.6	0.002	0.993	0.23	0.078	0.72	0.990	0.34	14.0	0.002	0.981	0.993	0.25	8.7	-40.8	1.38	0.993	0.26

Table S4. Nonlinear model fits for adsorption of ten aliphatic SOCs on HD3000

SOC	Langmuir				Freundlich				Langmuir-Freundlich					Polanyi-Manes models				
	q_m	K_L	r^2	RMSE	K_F	n	r^2	RMSE	q_m	K_S	n	r^2	RMSE	q_m	a	b	r^2	RMSE
TCE	32.0	0.017	0.982	0.91	1.300	0.61	0.994	0.53	541.8	7E-05	0.641	0.994	0.59	$_{193.1}$	-8.3	0.79	0.994	0.56
CCl_4	14.6	0.011	0.960	0.88	0.680	0.51	0.986	0.88	21.6	0.004	0.678	0.970	0.83	$_{14.1}$	-21.1	1.00	0.970	0.83
PCE	34.7	0.103	0.993	0.59	3.721	0.68	0.998	0.21	135.3	0.007	0.705	0.999	0.18	$_{86.3}$	-17.3	1.65	0.999	0.17
111TCA	14.8	0.004	0.994	0.24	0.178	0.69	0.996	0.18	32.5	0.001	0.755	0.998	0.15	$_{17.1}$	-20.2	1.25	0.998	0.15
11DCE	11.4	0.006	0.969	0.46	0.508	0.46	0.967	0.52	13.4	0.004	0.821	0.972	0.50	$_{11.1}$	-36.3	1.86	0.971	0.50
112TCA	23.0	0.007	0.949	1.16	0.712	0.55	0.990	0.76	311.7	3E-05	0.615	0.977	0.87	$_{1244}$	-6.4	0.45	0.942	1.39
12DBE	43.1	0.004	0.988	1.01	0.858	0.58	0.995	0.72	87.2	0.001	0.705	0.997	0.58	$_{65.1}$	-16.7	1.36	0.996	0.62
12DCP	25.0	0.003	0.967	0.99	0.539	0.52	0.967	0.71	79.9	2E-04	0.607	0.984	0.76	$_{29.5}$	-13.3	1.15	0.984	0.76
1112TeCA	36.4	0.009	0.980	1.39	1.444	0.52	0.995	0.82	65.4	0.002	0.633	0.999	0.27	$_{37.8}$	-20.5	1.35	0.999	0.29
DBCP	51.2	0.078	0.984	1.62	6.118	0.53	0.994	1.52	78.7	0.025	0.704	0.995	0.96	76.7	-40.9	1.81	0.995	1.02

38 **Table S5.** Nonlinear model fits for adsorption of ten aliphatic SOCs on SWCNT

SOC	Langmuir				Freundlich				Langmuir-Freundlich					Polanyi-Manes models				
	q_m	K_L	r^2	RMSE	K_F	n	r^2	RMSE	q_m	K_S	n	r^2	RMSE	q_m	a	b	r^2	RMSE
TCE	31.7	0.007	0.962	1.77	1.275	0.50	0.987	0.80	133.8	1E-04	0.499	0.993	0.82	35.2	-9.4	1.11	0.993	0.82
CCl_4	17.2	0.085	0.856	2.76	3.155	0.30	0.939	0.78	93.2	2E-05	0.297	0.988	0.86	21.8	-4.8	1.00	0.988	0.84
PCE	42.6	0.076	0.976	1.91	4.795	0.52	0.970	2.14	55.8	0.034	0.699	0.991	1.27	42.9	-31.6	1.65	0.991	1.27
111TCA	10.5	0.066	0.886	1.01	2.865	0.22	0.983	0.49	19.5	0.004	0.356	0.980	0.48	12.2	-8.6	1.38	0.980	0.05
11DCE	10.7	0.004	0.811	1.22	0.672	0.36	0.967	0.72	68.4	2E-05	0.456	0.927	0.82	60.0	-2.6	0.31	0.967	0.55
112TCA	21.8	0.005	0.983	0.81	0.751	0.48	0.993	0.71	34.2	0.001	0.654	0.996	0.40	25.5	-20.3	1.53	0.996	0.44
12DBE	20.2	0.034	0.862	2.85	2.461	0.36	0.942	0.96	141.8	2E-05	0.357	0.983	1.08	47.6	-4.9	0.93	0.984	1.04
12DCP	15.0	0.003	0.977	0.59	0.218	0.60	0.946	0.91	15.0	0.003	0.994	0.977	0.63	13.0	-88.2	1.99	0.976	0.64
1112TeCA	27.4	0.027	0.775	4.66	3.913	0.33	0.964	2.15	250.4	1E-05	0.383	0.947	2.47	424.1	-3.2	0.27	0.983	1.39
DBCP	35.3	0.102	0.918	3.30	7.373	0.32	0.971	1.66	54.9	0.019	0.493	0.998	0.51	42.2	-23.0	1.70	0.999	0.48

Table S6. Freundlich isotherm parameters of aliphatic SOCs adsorption in DDW

SOC	Adsorbent	$K_{F\mu}$ [a] $(mg/g)/(\mu g/L)^n$	K_{Fm} [a] $(mg/g)/(mg/L)^n$	Q [b] mg/m^2	n	r^2
TCE	SWCNT	1.2748	39.6	0.074	0.50	0.987
	HD3000	1.3002	87.9	0.137	0.61	0.994
	GNS	0.0320	12.3	0.018	0.86	0.996
	rGO	0.0110	7.7	0.015	0.95	0.984
CCl_4	SWCNT	3.1549	25.9	0.048	0.30	0.939
	HD3000	0.6800	22.6	0.035	0.51	0.986
	GNS	0.0392	11.5	0.017	0.82	0.984
	rGO	0.0139	4.1	0.008	0.82	0.992
PCE	SWCNT	4.7953	172.5	0.321	0.52	0.970
	HD3000	3.7205	416.1	0.648	0.68	0.998
	GNS	0.2871	52.8	0.079	0.75	0.995
	rGO	0.0955	27.2	0.055	0.82	0.989
111TCA	SWCNT	2.8651	13.2	0.025	0.22	0.983
	HD3000	0.1775	21.0	0.033	0.69	0.996
	GNS	0.0047	9.1	0.014	1.09	0.982
	rGO	0.0012	2.9	0.006	1.13	0.991
11DCE	SWCNT	0.6721	8.4	0.016	0.36	0.967
	HD3000	0.5080	12.2	0.019	0.46	0.967
	GNS	0.0033	4.7	0.007	1.05	0.990
	rGO	0.0006	2.2	0.004	1.18	0.992
112TCA	SWCNT	0.7508	21.1	0.039	0.48	0.993
	HD3000	0.7122	32.1	0.050	0.55	0.990
	GNS	0.0086	5.2	0.008	0.93	0.987
	rGO	0.0008	4.0	0.008	1.24	0.994
12DBE	SWCNT	2.4611	29.9	0.056	0.36	0.942
	HD3000	0.8581	47.8	0.074	0.58	0.995
	GNS	0.0023	6.6	0.010	1.15	0.983
	rGO	0.0012	9.0	0.018	1.30	0.991
12DCP	SWCNT	0.2183	13.7	0.025	0.60	0.946
	HD3000	0.5394	19.5	0.030	0.52	0.967
	GNS	0.0026	5.0	0.008	1.10	0.997
	rGO	0.0013	2.2	0.004	1.07	0.998
1112TeCA	SWCNT	3.9129	37.5	0.070	0.33	0.964
	HD3000	1.4443	51.1	0.080	0.52	0.995
	GNS	0.0350	11.2	0.017	0.84	0.987
	rGO	0.0085	8.8	0.018	1.00	0.999
DBCP	SWCNT	7.3732	69.3	0.129	0.32	0.971
	HD3000	6.1177	234	0.364	0.53	0.994
	GNS	0.0165	9.8	0.015	0.92	0.985
	rGO	0.0781	11.4	0.023	0.72	0.990

[a] Mass-basis adsorption affinity expressed in different units; [b] Surface area normalized adsorption capacity.

Table S7. Freundlich isotherm parameters of aliphatic SOCs adsorption in NOM preloading conditions

SOC	Adsorbent	$K_{F\mu}$ [a] (mg/g)/(μg/L)^n	K_{Fm} [a] (mg/g)/(mg/L)^n	R_u [b]	R_m [c]	n	r^2
TCE	SWCNT-DDW	1.2748	39.6	--	--	0.50	0.987
	SWCNT-NOM	0.8801	13.2	0.69	0.33	0.39	0.981
	GNS-DDW	0.0320	12.3	--	--	0.86	0.996
	GNS-NOM	0.0076	7.9	0.24	0.64	1.01	0.976
	rGO-DDW	0.0110	7.7	--	--	0.95	0.984
	rGO-NOM	0.0152	6.2	1.38	0.81	0.87	0.993
PCE	SWCNT-DDW	4.7953	172.5	--	--	0.52	0.970
	SWCNT-NOM	2.3521	45.5	0.49	0.26	0.43	0.990
	GNS-DDW	0.2871	52.8	--	--	0.75	0.995
	GNS-NOM	0.0446	21.8	0.16	0.41	0.90	0.990
	rGO-DDW	0.0955	27.2	--	--	0.82	0.989
	rGO-NOM	0.1377	19.5	1.44	0.72	0.72	0.993
11DCE	SWCNT-DDW	0.6721	8.4	--	--	0.36	0.967
	SWCNT-NOM	0.0341	5.4	0.05	0.64	0.73	0.976
	GNS-DDW	0.0033	4.7	--	--	1.05	0.990
	GNS-NOM	0.0006	2.6	0.18	0.55	1.21	0.997
	rGO-DDW	0.0006	2.2	--	--	1.18	0.992
	rGO-NOM	0.0006	2.0	1.00	0.91	1.17	0.997
112TCA	SWCNT-DDW	0.7508	21.1	--	--	0.48	0.993
	SWCNT-NOM	0.1372	7.1	0.18	0.34	0.57	0.967
	GNS-DDW	0.0086	5.2	--	--	0.93	0.987
	GNS-NOM	0.0022	2.9	0.26	0.56	1.04	0.995
	rGO-DDW	0.0008	4.0	--	--	1.24	0.994
	rGO-NOM	0.0007	3.6	0.88	0.90	1.24	0.983
1112TeCA	SWCNT-DDW	3.9129	37.5	--	--	0.33	0.964
	SWCNT-NOM	0.9489	11.4	0.24	0.30	0.36	0.977
	GNS-DDW	0.0350	11.2	--	--	0.84	0.987
	GNS-NOM	0.0050	7.7	0.14	0.68	1.06	0.994
	rGO-DDW	0.0085	8.8	--	--	1.00	0.999
	rGO-NOM	0.0074	7.4	0.87	0.84	1.00	0.994
DBCP	SWCNT-DDW	7.3732	69.3	--	--	0.32	0.971
	SWCNT-NOM	1.1402	27.0	0.15	0.39	0.46	0.994
	GNS-DDW	0.0165	9.8	--	--	0.92	0.985
	GNS-NOM	0.0048	6.0	0.29	0.61	1.03	0.996
	rGO-DDW	0.0781	11.4	--	--	0.72	0.990
	rGO-NOM	0.1008	8.8	1.29	0.77	0.65	0.975

[a] Mass-basis adsorption affinity expressed in different units; [b] K_F ratio of SOCs in NOM preloading adsorption to that in DDW at equilibrium concentration of 1μg/L; [c] K_F ratio of SOCs in NOM preloading adsorption to that in DDW at equilibrium concentration of 1mg/L.

47

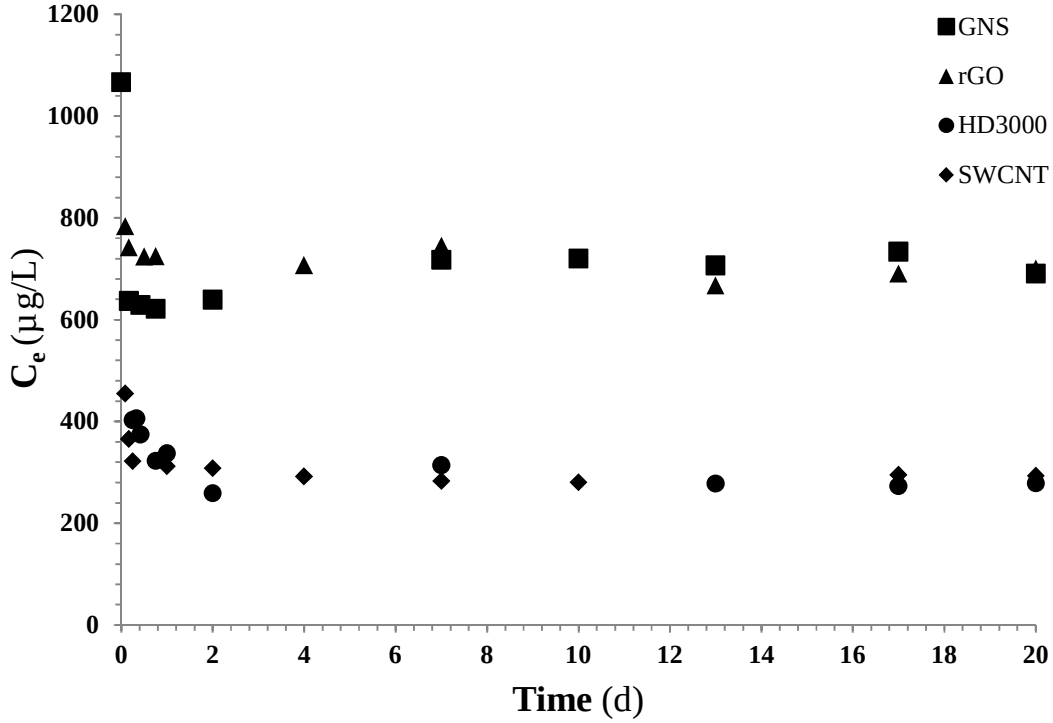

48

49 **Figure S1.** Adsorption kinetics of TCE onto GNS, rGO, HD3000 and SWCNT in DDW.

50

51

52

53

54

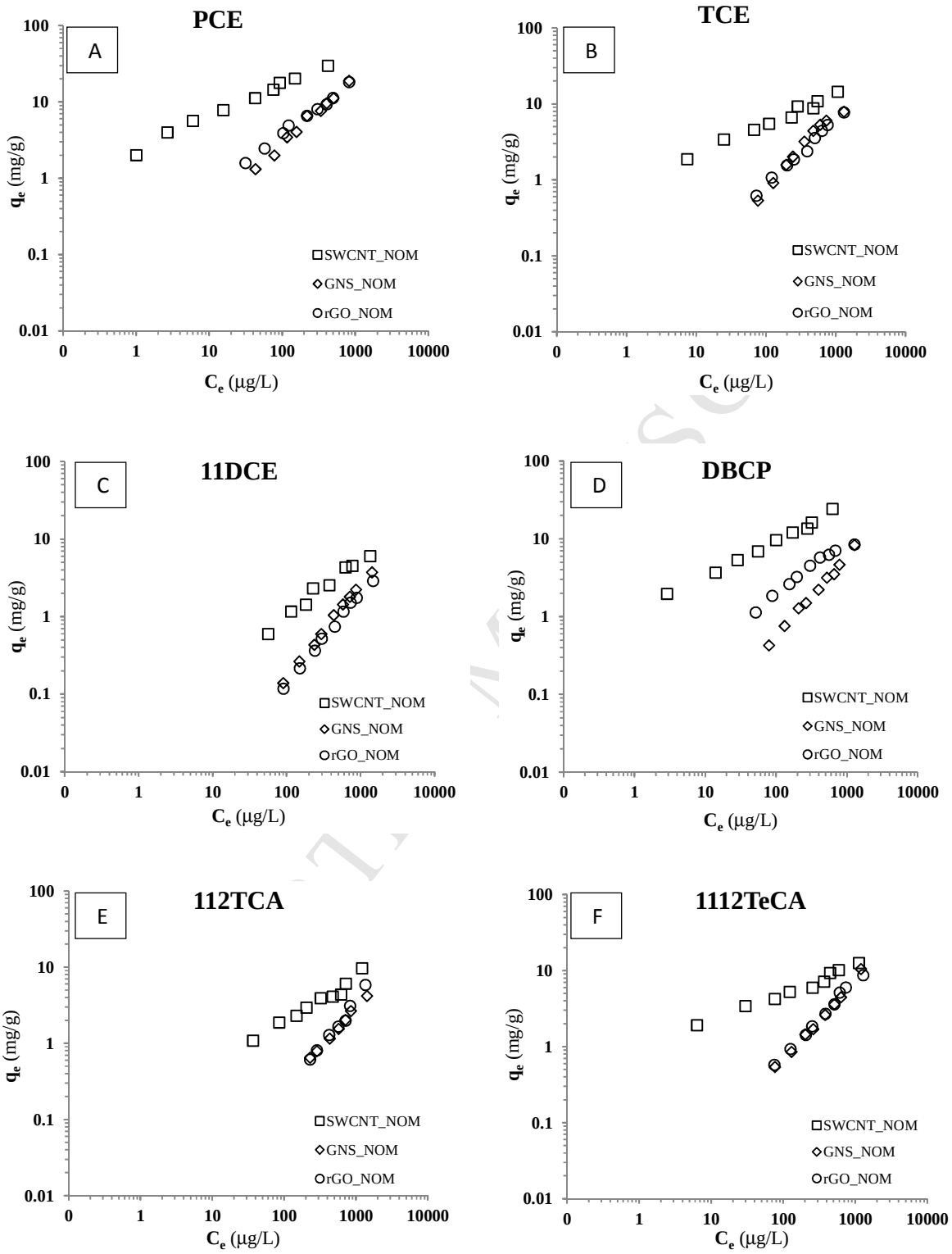

Figure S2. Adsorption isotherms under NOM preloading conditions (A) PCE, (B) TCE, (C) 11DCE, (D) DBCP, (E) 112TCA, and (F) 1112TeCA.

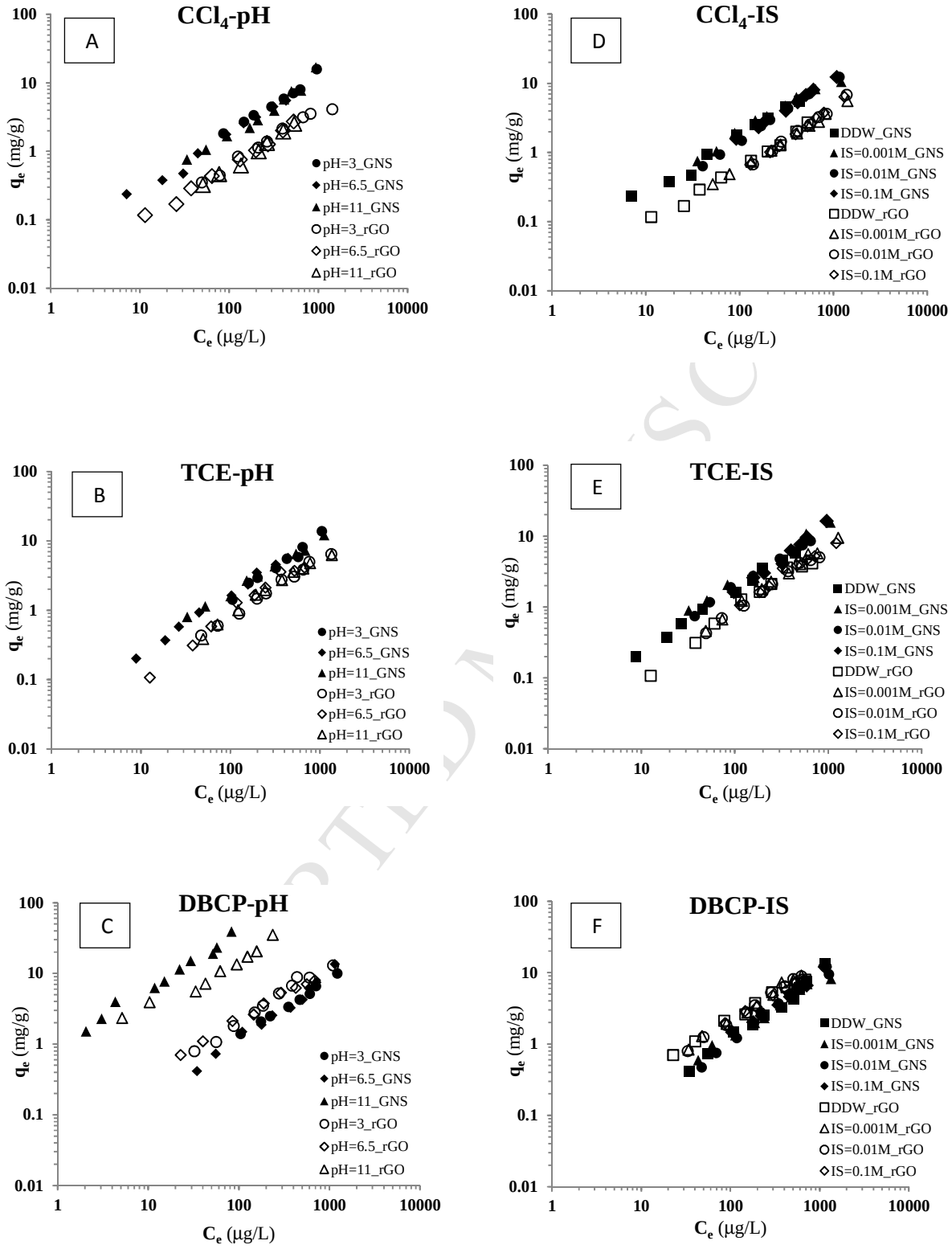

Figure S3. Adsorption isotherms in different solution pH and IS (A) CCl_4-pH, (B) TCE-pH, (C) DBCP-pH, (D) CCl_4-IS, (E) TCE-IS, and (F) DBCP-IS.